

Multiple phase gratings in pure, Yb- and P-doped $\text{Pb}_5\text{Ge}_3\text{O}_{11}$ after different thermal treatments

Xuefeng Yue,^{a)} S. Mendricks, T. Nikolajsen,^{b)} H. Hesse, D. Kip, and E. Krätzig
Fachbereich Physik der Universität Osnabrück, Barbarastr.7, D-49069 Osnabrück, Germany

(Received 15 October 1998; accepted for publication 29 April 1999)

Multiple phase gratings are written in pure, Yb- and P-doped $\text{Pb}_5\text{Ge}_3\text{O}_{11}$ crystals: a fast grating and a slow grating with substantially different response times compensate each other. Doping and thermal treatments have strong influences on the behavior of both gratings. Reduction treatments of Yb-doped samples lead to a significant decrease of the response time of the slow grating, while that of the fast grating is diminished by more than two orders of magnitude. P doping significantly increases the response time of the fast grating. Possible origins of both gratings are discussed.

© 1999 American Institute of Physics. [S0021-8979(99)09915-6]

I. INTRODUCTION

The photorefractive effect in electro-optic crystals arises from a charge redistribution under illumination which causes a change of the refractive index via the electro-optic effect.¹ In a photorefractive material, the maximum modulation of the refractive index is a main parameter to describe the photorefractive effect. Furthermore, this modulation is of importance for holographic applications.² When diffusion is the dominant charge transport mechanism, this parameter is mainly determined by the effective electro-optic coefficient and the effective charge density.³ If two types of charge carriers (electrons and holes) are involved in the charge transport process, electron-hole competition further limits the maximum modulation of the refractive index.^{4,5} In addition, the involvement of different charge carriers in holographic recording may cause multiple gratings and grating compensation, which have been found in most photorefractive crystals.⁶ In some cases, the multiple gratings are of importance, e.g., for nondestructive or quasiconstructive readout of the recorded gratings.⁷⁻⁹ Only after the full understanding of the multiple gratings involved in holographic recording, can one find a way to control them and use them for practical applications.

Ferroelectric lead germanate ($\text{Pb}_5\text{Ge}_3\text{O}_{11}$) crystals possess relatively large electro-optic coefficients.¹⁰ At room temperature $\text{Pb}_5\text{Ge}_3\text{O}_{11}$ belongs to the point group 3. It has been demonstrated recently that holographic recording and beam coupling can be realized in this material.^{11,12} At an intensity of 0.5 W/cm^2 , a fast grating with a response time less than 1 s and a slow grating with a time constant of several hours can be formed. Both of them are refractive index gratings. In Ref. 12, the fast gratings in lead germanate crystals have been studied systematically. It has been demonstrated that the maximum diffraction efficiencies of the fast gratings in all samples are generally much smaller than

the theoretically predicted values. This difference has been attributed to electron-hole competition. The slow grating in a pure sample, however, has a much larger amplitude. In this contribution, we focus on multiple gratings in pure and doped $\text{Pb}_5\text{Ge}_3\text{O}_{11}$ crystals. Both as-grown and thermally treated samples are used in the present experiments. In the second section, we describe the basic experimental arrangement and the samples used for the investigations. Then, we present results on grating formation and decay in different samples. Characteristic time constants are measured, and the behavior of decay with and without homogeneous illumination is studied. In the last part, we compare and discuss the results.

II. EXPERIMENTAL ARRANGEMENT AND SAMPLES

A holographic setup is used to measure the photorefractive properties of lead germanate crystals: Two expanded beams of an Ar^+ laser (wavelength $\lambda = 488 \text{ nm}$) of approximately equal intensity (modulation depth $m_0 > 0.98$) and extraordinary polarization are used to write gratings with grating vectors parallel to the c axis of the crystals. The total intensity of the writing beams is 0.6 W/cm^2 . The grating formation is monitored by a weak extraordinarily polarized He-Ne laser beam ($\lambda = 633 \text{ nm}$) incident at the Bragg angle. This red probe beam is not expanded and its intensity is 0.3 W/cm^2 . Both diffracted and transmitted probe beam intensities are measured, and the diffraction efficiency is defined as the ratio between the diffracted and the sum of diffracted and transmitted beam intensity. During the reading process, both writing beams are turned off. Optical erasure is performed by one of the writing beams. The grating spacing is $1.2 \mu\text{m}$ unless otherwise specified.

The $\text{Pb}_5\text{Ge}_3\text{O}_{11}$ crystals have been grown by the Czochralski method at the Crystal Growth Laboratory of the University of Osnabrück. The description of the samples is presented in Table I. Nominally pure, P- and Yb-doped crystals are cut, polished to optical quality, and poled to single-domain state. During poling, the samples are heated to temperatures slightly above the phase transition temperature T_C ($T_C \sim 180^\circ \text{C}$ for pure $\text{Pb}_5\text{Ge}_3\text{O}_{11}$) and cooled down to room

^{a)}Present address: California Institute of Technology, MS 136-93, Pasadena, California 91125; electronic mail: yxuefeng@optics.caltech.edu

^{b)}Risø National Laboratory, Optics and Fluid Department, DK-4000 Roskilde, Denmark.

TABLE I. Descriptions of our samples used in the experiments. (Absorption coefficients are measured for wavelength $\lambda = 488$ nm and extraordinarily polarized light.)

Symbol	Crystal and dopant	Dimensions [$a \times b \times c$ (mm ³)]	Absorption coefficient α_e (cm ⁻¹)
PGO-AG	As-grown PGO(Pb ₅ Ge ₃ O ₁₁)	2.40×6.20×5.50	3.2
PGO-RED	Reduced PGO	2.40×5.12×5.75	3.0
Yb50-AG	As-grown PGO: 50 ppm Yb	2.95×4.75×7.45	3.1
Yb50-OX	Oxidized Yb50	2.30×3.30×4.15	3.1
Yb50-RED	Reduced Yb50	2.25×3.15×3.80	1.4
P200-AG	As-grown PGO: 200 ppm P	2.60×5.15×7.00	1.6
P200-OX	Oxidized P200	2.55×4.95×7.60	1.6
P200-RED	Reduced P200	2.55×4.95×7.15	1.3

temperature under an electric field of about 0.3 kV/cm. Two kinds of thermal treatments (reduction and oxidation) are carried out for some samples. For reduction, the samples are heated to 350 °C in an atmosphere of 20% H₂ and 80% N₂ for about 1 h, whereas for oxidation, they are heated up to 600 °C in pure O₂ for about 5 h. After these treatments, another poling procedure must be carried out. It is well known that some dopants can greatly influence the property of most photorefractive crystals. But the effects of the same dopant may be substantially different in various host materials, e.g., cerium can increase the performance of strontium barium niobate,¹³ while it is not an effective dopant in lithium niobate.¹⁴ We have tested various dopants in lead germanate. Here, we report the results of P- and Yb-doped samples because of their representative effects.

The absorption spectrum of a nominally pure sample has been presented in our previous paper.¹² In Table I we list the absorption coefficients of different samples at wavelength $\lambda = 488$ nm. Yb dopant has almost no influence on the absorption spectrum, but P dopant leads to a significant decrease of the absorption coefficients in wavelength range $\lambda < 550$ nm. Reduction of Yb-doped samples makes the absorption smaller, while oxidation does not induce any observable change in the absorption. The refractive indices for 633 nm are $n_e(633 \text{ nm}) = 2.148$ and $n_o(633 \text{ nm}) = 2.113$, and those for 488 nm are $n_e(488 \text{ nm}) = 2.215$ and $n_o(488 \text{ nm}) = 2.178$, respectively.¹⁵ The linear electro-optic coefficients r_{13} and r_{33} are fairly large with values of 10.5 and 15.3 pm/V, respectively.¹⁰ Another useful parameter is the dielectric constant $\epsilon_{33} = 40$.

III. EXPERIMENTS RESULTS

A. Gratings in nominally pure samples

The writing and decay cycle in the nominally pure as-grown sample (PGO-AG) is shown in Fig. 1. After both writing beams are turned on, the fast grating forms in less than 1 s. If we continue writing, the measured diffraction efficiency decreases gradually to zero and then, increases again to a saturation value in about 2 h (region A in Fig. 1). The shutdown of both writing beams leads to an abrupt rise of the diffraction efficiency (region B) and a further increase occurs when homogeneous illumination is present (region C). The fast and the slow gratings are 180° out of phase and partially compensate each other. The maximum measured

refractive-index modulation corresponding to the fast grating is $\Delta n_f = 1 \times 10^{-5}$, while that for the slow grating is $\Delta n_s = 3.4 \times 10^{-5}$.

For the fast grating, the decay probed by the He-Ne laser beam leads to a time constant of $\tau_d^f = 0.64$ s, and with an additional optical erasure beam of wavelength 488 nm and intensity 0.3 W/cm² to $\tau_p^f = 0.16$ s. The decay time constant for the slow grating, however, is much larger than that of the fast one, and we get $\tau_d^s = 1.2 \times 10^5$ s and $\tau_p^s = 1.9 \times 10^4$ s, respectively. Here, the superscripts *f* and *s* denote fast and slow gratings, respectively, and the subscripts *p* and *d* denote the erasure with and without blue light. We regard the decay probed only by the He-Ne laser beam as dark decay because of the extremely small absorption of all samples at 633 nm [$\alpha_e(633 \text{ nm}) < 0.4 \text{ cm}^{-1}$], while that with the presence of the 488 nm illumination is called optical erasure.

The reduction treatment of the nominally pure sample does not lead to a significant change in the response time of the fast grating. The decay time constants, for example, are $\tau_d^f = 0.86$ s and $\tau_p^f = 0.18$ s for the fast grating. The dark decay time constant of the slow grating is measured to be $\tau_d^s = 1.8 \times 10^4$ s, while it is $\tau_p^s = 4.5 \times 10^3$ when the illumination beam (488 nm) is present. Clearly, the reduction of the sample leads to a faster response of the slow grating.

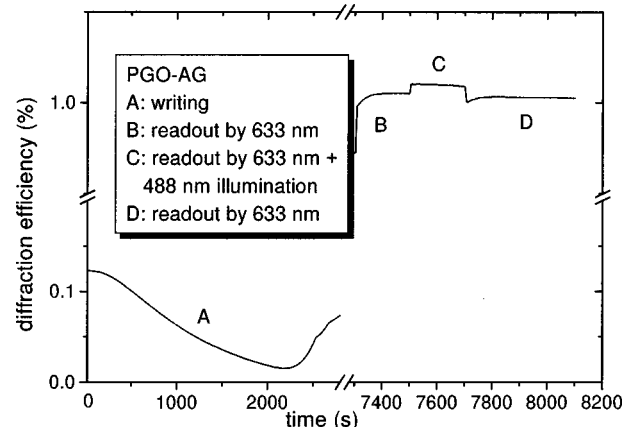


FIG. 1. Recording and decay behavior of the nominally pure Pb₅Ge₃O₁₁ (PGO-AG). Wavelength and intensity of the writing beams are $\lambda = 488$ nm and $I_0 = 0.6 \text{ W/cm}^2$, and grating spacing is $\Lambda = 1.2 \mu\text{m}$. Wavelength and intensity of the illumination beam are $\lambda = 488$ nm and $I_E = 0.3 \text{ W/cm}^2$.

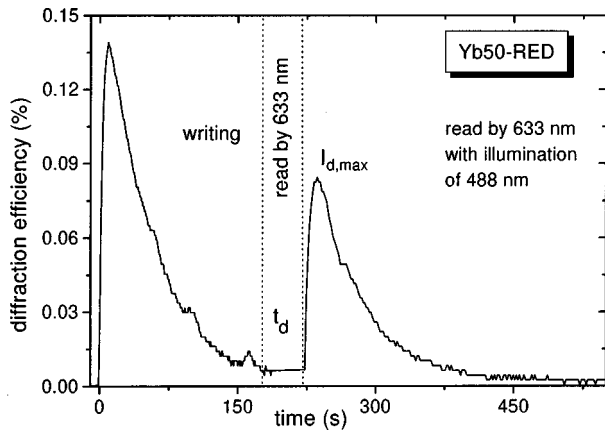


FIG. 2. Recording and decay behavior of the reduced Yb-doped $\text{Pb}_5\text{Ge}_3\text{O}_{11}$ (Yb50-RED). The experimental conditions are the same as those in Fig. 1. The slow grating compensates completely for the fast grating in 200 s. The diffraction efficiency remains approximately zero if the gratings are probed only by a He-Ne laser beam. With the presence of homogeneous illumination (488 nm), the slow grating is revealed, and then gradually decays to zero.

B. Gratings in Yb-doped samples

An as-grown Yb-doped sample (Yb50-AG) is also used for holographic recording. Again, for a short-time recording, only a fast grating is formed. The time constant for dark decay is $\tau_d^f = 0.76$ s while that for optical erasure is $\tau_p^f = 0.24$ s. In this sample, the formation of the slow grating becomes faster than in the PGO-AG sample. The time constant of the slow grating for dark decay is $\tau_d^s = 2.0 \times 10^4$ s, while that for the erasure with illumination is $\tau_p^s = 7.0 \times 10^3$ s. No change in saturated refractive-index modulation of the fast grating has been observed compared to the pure sample.

The writing and decay cycle of holographic recording in the reduced sample (Yb50-RED) is presented in Fig. 2. In this sample, the response time of the fast grating becomes much larger compared to that in the as grown crystal. The decay time constants for the fast grating are $\tau_d^f = 23.0$ s and $\tau_p^f = 3.86$ s. Note that the slow grating can completely compensate for the fast grating in about 200 s. This means the reduction decreases the response time of the slow grating. Then both gratings cancel each other and the diffraction efficiency remains zero even for several hours of recording. If the recorded gratings are probed by the He-Ne laser beam alone, diffraction efficiency remains at about zero. With the presence of the illumination beam the diffraction efficiency to a maximum value and then decays slowly to zero.

It is not possible to measure the decay time constant by using only a He-Ne laser beam, because the fast and slow gratings always compensate each other. We use the following way to measure the decay time constant of the slow grating: after a recording time of 100 s, the gratings are probed by the He-Ne beam and then the illumination beam is turned on after a time interval t_d . With illumination, the decay time constant of the slow grating is 85 s which is much larger than that of the fast grating. The maximum revealed diffraction efficiency after turning on the illumination beam can be regarded as that of the remaining slow grating

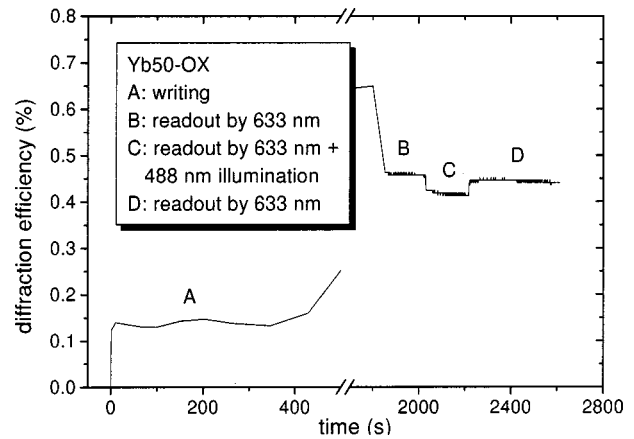


FIG. 3. Recording and decay behavior of the oxidized Yb-doped $\text{Pb}_5\text{Ge}_3\text{O}_{11}$ (Yb50-OX). The experimental conditions are the same as those in Fig. 1. In the reading mode, homogeneous illumination is first present and then turned off. The turnoff of the illumination beam leads to a small increase in the diffraction efficiency.

after the t_d decay probed by the He-Ne beam. By these measurements, we get a dark decay time constant τ_d^s of approximately 580 s.

The holographic recording and erasure cycle for the oxidized sample (Yb50-OX) is presented in Fig. 3. Unlike the as-grown and reduced samples, the slow and fast gratings in Yb50-OX are in phase. To check this carefully, we measure the intensities of both interacting beams. There is no change of energy transfer direction at the initial and final states during holographic recording. Under the same conditions as described above, the dark decay time constant of the fast grating is $\tau_d^f = 0.70$ s and that with illumination $\tau_p^f = 0.18$ s. The decay time constants of the slow grating, however, are larger than those of Yb50-AG: $\tau_d^s = 2.2 \times 10^5$ s and $\tau_p^s = 1.4 \times 10^4$ s.

Oxidation increases the efficiency of the slow grating in Yb-doped samples. For example, after a recording for 2 h, the ratio between the efficiencies of the slow and fast gratings is $\eta_S/\eta_F = 3.0$ for Yb50-AG, and $\eta_S/\eta_F = 5.0$ for Yb50-OX.

C. Gratings in P-doped samples

For P-doped $\text{Pb}_5\text{Ge}_3\text{O}_{11}$, we have also measured the response time constants of the fast grating in as-grown, oxidized, and reduced samples. There is no significant difference among them (see Table II). The values, however, are larger than those of the pure samples as well as those of the as-grown and oxidized Yb-doped samples. But, they are still much smaller than the corresponding response time of the reduced Yb-doped sample. Like in the nominally pure samples, reduction leads to a faster response of the slow grating, although the effect is not as large as that in the Yb-doped samples. Again, P dopant does not change the refractive-index modulation of the fast grating. The saturated refractive-index modulation can reach a value several times larger than that of the fast grating.

TABLE II. Decay time constants of the fast and slow gratings τ_d^f , τ_d^s probed by a He-Ne laser (wavelength 633 nm and intensity 0.3 W/cm²) alone and with the presence of an illumination beam τ_p^f , τ_p^s (wavelength 488 nm and intensity 0.3 W/cm²).

Sample	τ_d^f	τ_p^f	τ_d^s	τ_p^s
PGO-AG	0.64 s	0.16 s	1.2×10^5 s	1.9×10^4 s
PGO-RED	0.86 s	0.18 s	1.8×10^4 s	4.5×10^3 s
Yb50-AG	0.76 s	0.24 s	2.0×10^4 s	7.0×10^3 s
Yb50-OX	0.70 s	0.18 s	2.2×10^5 s	1.4×10^4 s
Yb50-RED	23.0 s	3.86 s	580 s	85 s
P200-AG	8.4 s	1.2 s	3.5×10^3 s	1.7×10^3 s
P200-OX	5.0 s	0.8 s	1.1×10^4 s	4.3×10^3 s
P200-RED	11.0 s	1.4 s	1.6×10^3 s	1.1×10^3 s

D. Summary of experimental results

For comparison of the decay time constants of the fast and slow gratings in different samples, we have listed all measured values in Table II. The main results concerning time constants and grating amplitudes are summarized as follows:

(1) The time constant of the fast grating in the pure sample is at least four orders of magnitude smaller than that of the slow grating.

(2) P doping enlarges the time constant of the fast grating substantially, while Yb doping has little influence on the fast grating.

(3) Reduction of the Yb-doped sample leads to a significant increase of the time constant of the fast grating and to a large decrease of the time constant of the slow grating.

(4) The amplitude of the fast grating is not influenced by doping and thermal treatments. The typical value is $\Delta n_f = 1 \times 10^{-5}$ for a grating spacing of $\Lambda = 1.2 \mu\text{m}$.

(5) In all as-grown and oxidized samples, the modulation of the refractive index of the slow grating can reach a much larger value, even ten times as high as that of the fast grating. Reduction treatments, however, lower the amplitude of the slow grating in doped samples.

IV. DISCUSSION

The photorefractive effect is related to photoionization and transport of charge carriers. The space-charge field under sinusoidal illumination without an externally applied electric field and in the absence of a photovoltaic field can be expressed as¹⁶

$$E_{sc} = iRmE_D / (1 + E_D/E_Q), \quad (1)$$

where m is the effective modulation depth influenced by dark conductivity σ_d and photoconductivity σ_p and proportional to the modulation depth m_0 of the recording intensity:

$$m = m_0 / (1 + \sigma_d/\sigma_p). \quad (2)$$

Here R is electron-hole competition constant.⁵ Furthermore,

$$E_D = Kk_B T/e, \quad \text{and} \quad E_Q = eN_E / (\epsilon\epsilon_0 K) \quad (3)$$

are the diffusion and limiting space-charge fields, respectively. Here K is the magnitude of the grating vector, k_B the Boltzmann constant, T the temperature, e the charge of electron, $\epsilon\epsilon_0$ the static dielectric constant, and N_E the effective

photorefractive charge density: $1/N_E = 1/N_A + 1/N_D$, where N_A is the density of acceptors and N_D is the density of donors.

A. Properties of the fast grating

The amplitudes of the fast gratings in all samples used here are much smaller than the theoretical predictions based on diffusion field and electro-optic coefficients. This has been shown in detail in Ref. 12. Many factors can limit the amplitude of photorefractive gratings, e.g., electron-hole competition [see Eq. (1)], shallow trap effects,¹⁷ non-negligible dark conductivity [Eq. (2)], degradation of the interference pattern,¹⁸ etc. The off-Bragg readout can also reduce the measured diffraction efficiency. In this work, the dark conductivity can be neglected compared to photoconductivity. As reported in our previous paper,¹² the measured diffraction efficiency of the slow grating in the sample PGO-AG is in agreement with the theoretical prediction (off-Bragg factor can be excluded). The efficiency ratio between the slow and fast gratings (η_s/η_f) can reach 10 in the nominally pure sample. Normally a shallow trap effect cannot introduce such a large difference.¹⁷ So, we think the main factor to limit the amplitude of the fast grating is electron-hole competition.

As we have discussed in Ref. 12, doping does not enhance the photorefractive effect in $\text{Pb}_5\text{Ge}_3\text{O}_{11}$. We think that the photoactive centers are the intrinsic defects in this material. The main charge carriers involved in the fast grating are holes in all samples. This has been confirmed by two-beam coupling measurements in our experiments. It has been determined by electron spin resonance (ESR) measurements that after illumination of the nominally pure sample, both Pb^{2+} and Pb^{3+} ions exist in this material, while most of the Pb^{3+} ions disappear immediately after shutoff of the illumination.¹⁹ It is believed that by illumination, electrons can be excited from the valence band to the conduction band or to other defect centers. The remaining holes can move in the valence band and combine with Pb^{2+} to form Pb^{3+} . Based on these results, we think this process may be responsible for the formation of the fast grating. In this case, thermal treatments do not lead to any change of the fast grating. In P-doped samples, the response time constants of the fast gratings become much larger than those for all nominally pure samples. Yb doping, however, does not influence the fast grating significantly. We think this is reasonable by considering the much smaller absorption coefficients of the P-doped samples.

B. Properties of the slow grating

In all as-grown and reduced samples, the slow grating is 180° out of phase with respect to the fast grating. This indicates that the carriers responsible for the slow grating are negatively charged. First, we can conclude that these charge carriers are photoexcited. From the experimental results we know that the response of the slow grating strongly depends on thermal treatments. It is well known that oxygen vacancies can act as electron donors.¹⁶ It is possible that oxygen vacancies or some impurity ions adjoining oxygen vacancies, which can be influenced by thermal treatments, are respon-

sible for the formation of the slow grating. Doping with Yb and P influences the slow grating, but the thermal treatments of Yb-doped samples lead to some interesting changes of the recording behavior. Oxidization causes a change of main charge carriers and reduction leads to a significant decrease of the response time constant. Perhaps the valence state of Yb can be altered by a charge transfer to an adjoining oxygen vacancy. Therefore, in Yb-doped samples Yb^{3+} or Yb^{2+} may be connected with the slow grating. However, the observation that the amplitude of the slow grating decreases after the reduction treatments cannot be explained at this point of time.

C. Decay behavior of the slow grating

The decay behavior of the slow grating with and without homogeneous illumination as presented in Fig. 1 can be explained as follows: During writing, the fast grating is 180° out of phase with respect to the slow grating. After both writing beams are turned off, the decay of the fast grating causes an increase of the overall diffraction efficiency. In reading mode, we think that the charge carriers responsible for the fast grating move under the space-charge field of the slow grating to compensate it. Therefore, we call these charge carriers compensation charges. There are two forces which can move these compensation charges, i.e., drift and diffusion. In the dark, the decay of the fast grating stops when drift and diffusion get to a balanced state. This means that after the decay there are some charge carriers which compensate for the slow grating. With an intense homogeneous illumination, most of these compensation charge carriers are excited and diffusion becomes dominant, causing a new equilibrium state. This leads to a rise in the diffraction efficiency. After the shutoff of the intense illumination beam, the compensation charge carriers drift again in the space-charge field and compensate for the slow grating to some extent.

If the fast and slow gratings are in phase with each other, drift and diffusion forces are in the same direction so that the fast grating disappears after both writing beams are turned off. The intense illumination, however, can excite some charges which may drift in the remaining space-charge field and compensate the slow grating. Only with the illumination, there are enough free charge carriers for compensation.

Finally, we should mention that very low intensities of writing beams are used in our present experiments. We have also tried to use intensities of about 8 W/cm^2 to record gratings in the oxidized Yb-doped samples. The diffraction efficiency can reach values which are five times larger than that of the fast grating in about 2 min. The slow gratings decays in the dark with a time constant of about two days. Even with an erasure beam (wavelength $\lambda = 488 \text{ nm}$ and intensity $I = 0.3 \text{ W/cm}^2$) the slow grating can hold for about 4 h.

In conclusion, multiple gratings can be formed in photorefractive $\text{Pb}_3\text{Ge}_3\text{O}_{11}$ crystals. Doping and thermal treatments can greatly change the response of the gratings. The results can be summarized as follows:

(1) Slow gratings have generally much larger amplitudes and time constants than fast gratings. Electron-hole competition is the main factor which limits the amplitudes of fast gratings.

(2) The time constant of the fast grating is substantially enlarged by P doping.

(3) Yb doping has no influence on the response of the fast grating. Reduction of Yb-doped samples leads to an increase of about 30 times in the response time constant of the fast grating and lowers the time constant of the slow grating by about two orders of magnitude. Oxidation changes the type of main charge carriers responsible for the slow grating.

It is likely that Pb^{2+} ions plus holes in the valence band are responsible for the fast grating. Oxygen vacancies and impurities adjoining these vacancies may be responsible for the slow gratings. For a better understanding of the multiple gratings, further experiments are needed to identify the photorefractive centers corresponding to the slow gratings. The results presented in this paper provide some ways like, e.g., doping or thermal treatments to control some photorefractive properties in lead germanate crystals.

ACKNOWLEDGMENTS

Financial support of the Deutsche Forschungsgemeinschaft (SFB 225, A1, A6) and the Friedrich-Ebert-Stiftung are gratefully acknowledged. One of the authors (X.Y.) is grateful to A. Adibi for useful discussions and comments.

- ¹D. M. Pepper, J. Feinberg, and N. V. Kukhtarev, *Sci. Am.* **263** (10), 62 (1990).
- ²F. S. Chen, *J. Appl. Phys.* **38**, 3418 (1967).
- ³J. Feinberg, D. H. Heiman, J. A. R. Tanguary, and R. W. Wellwarth, *J. Appl. Phys.* **51**, 1297 (1980).
- ⁴R. Orlovski and E. Krätzig, *Solid State Commun.* **27**, 1351 (1978).
- ⁵F. P. Strohkendl, J. M. C. Jonathan, and R. W. Hellwarth, *Opt. Lett.* **11**, 312 (1986).
- ⁶X. Yue, E. Krätzig, and R. A. Rupp, *J. Opt. Soc. Am. B* **15**, 2383 (1998).
- ⁷J. P. Herriau and J. P. Huignard, *Appl. Phys. Lett.* **49**, 1140 (1986).
- ⁸L. Arizmendi, *J. Appl. Phys.* **65**, 423 (1988).
- ⁹A. Delboulbe, C. Fromont, J. P. Herriau, S. Mallick, and J. P. Huignard, *Appl. Phys. Lett.* **55**, 713 (1989).
- ¹⁰*Landolt Börnstein—Numerical Data and Functional Relationships in Science and Technology, New Series, III/16*, editor in chief: K.-H. Hellwig (Springer, Berlin, 1981).
- ¹¹W. Królikowski, M. Cronin-Golomb, and B. S. Chen, *Appl. Phys. Lett.* **57**, 7 (1990).
- ¹²X. Yue, S. Mendricks, Y. Hu, H. Hesse, and D. Kip, *J. Appl. Phys.* **83**, 3473 (1998).
- ¹³K. Buse, U. van Stevendaal, R. Pankrath, and E. Krätzig, *J. Opt. Soc. Am. B* **13**, 1461 (1996).
- ¹⁴D. K. McMillen, T. D. Hudson, J. Wagner, and J. Singleton, *Optics Express* **2**, 491 (1998).
- ¹⁵M. Simon, F. Mersch, C. Kuper, S. Mendricks, S. Wevering, J. Imbrock, and E. Krätzig, *Phys. Status Solidi A* **159**, 559 (1997).
- ¹⁶S. Ducharme and J. Feinberg, *J. Opt. Soc. Am. B* **3**, 283 (1986).
- ¹⁷P. Tayebati and D. Mahgerefteh, *J. Opt. Soc. Am. B* **8**, 1053 (1991).
- ¹⁸U. van Stevendaal, K. Buse, H. Malz, H. Veenhuis, and E. Krätzig, *J. Opt. Soc. Am. B* **15**, 2868 (1988).
- ¹⁹H.-J. Reyher and M. Pape (private communication).